

COMPLEX CONDUCTIVITY MEASUREMENTS OF RESERVOIR PROPERTIES

Frank D. Börner,
Dresden Groundwater Research Center, Dresden, Germany

Abstract The frequency dependence of complex electrical conductivity in the IP frequency range (10^{-3} to 10^4 Hertz) has been investigated for a variety of shaly sandstones. The laboratory measurements were made with a computer controlled four-electrode system on plugs saturated and partially saturated with brine of different composition.

It has been found that the complex nature of the conductivity is caused solely by the capacitive behaviour of the interlayer region between the solid matrix and the electrolytic pore solution. The resulting main feature of the conductivity spectra is a constant negative phase angle over the investigated frequency range combined with a nearly identical power law frequency dependence of the real as well as the imaginary parts.

The frequency exponent is in the order of about 0 to 0.03. It is related to common IP-parameters. The relationships between the frequency exponent and reservoir properties are of special interest. The results of the study show that the frequency exponent is (1) proportional to the surface area to porosity ratio, (2) inversely proportional to water salinity, and (3) it shows a complicated dependence on water saturation.

Complex conductivity measurements enable an uncomplicated separation of electrical volume and interface effects to be made. Moreover, the results suggest that determination of specific surface area of reservoir rocks directly from complex electrical measurements can be made.

INTRODUCTION

Natural wet rocks are generally very heterogeneous multi phase systems with a complicated internal structure. They consist of a nonconductive silicate matrix and a more or less conductive electrolyte solution in the pore space.

Interactions at and near the contact area of the solid and liquid phases are the cause of the development of a phase boundary layer with unusual physical and chemical properties. Different electrical phase boundary phenomena are of special interest, because they result in a dispersion of the electrical conductivity in the frequency range from 1 mHz to 10 kHz.

Current problems include the determination of rock permeability, evaluation of fluid properties in the pore space (including type and concentration of contaminants) and the monitoring of corresponding parameters together with artificially induced changes of physical and chemical rock properties (redevelopment of contaminated groundwater reservoirs, underground cracking of rocks). Using for example Induced Polarization measurements, the complex electrical rock parameters such as frequency effect or phase angle can be obtained. They depend on pore space structure and microstructure of the internal rock boundary layer. Therefore, they contain information about rock permeability and present organic or inorganic contaminants. But use and application of their high information content is limited. On the one hand, technical problems exist. On the other, there is a lack of knowledge, of how complex electrical rock parameters are influenced at very low frequencies by pore space structure, fluid properties and interactions at and near the internal rock interface. Laboratory investigations can lead to a greater understanding of the fundamental relationships between reservoir properties and the dispersion of electrical parameters.

Laboratory measurements of complex conductivity related to porous rocks including the IP-frequency range are published for example by Olhoeft (1985), Lockner and Byerlee (1985) or Wiley and Snoddy (1986). Systematic investigations like the detailed publication of Vinegar and Waxman (1984) are seldom.

COMPLEX ROCK CONDUCTIVITY

When a time varying electrical field is applied to a rock sample, the structure and composition cause the simultaneous occurrence of a electrical conduction and a dielectric displacement current. On the basis of second Maxwell's law, which connects the two current components, and a sinusoidal time dependence of the electrical field, an effective conductivity σ^* is defined. This quantity is complex with frequency dependent real (σ') and imaginary part (σ'') and includes conduction as well as polarization mechanism (Olhoeft, 1979):

$$\sigma^*(\omega) = \sigma'(\omega) - i\sigma''(\omega) \quad (1)$$

ω is the angular frequency and i the imaginary unit. This is sensible, because in water bearing porous rocks charge carrier transport is the dominating electrical process, and at very low frequencies the measuring method is based on a conductivity measurement.

σ^* is related to the complex specific resistivity ρ^*

$$\rho^* = 1 / \sigma^* \quad (2)$$

The commonly primary measured quantities - resistivity magnitude $|\rho^*|$ and phase angle φ - are connected with the conductivity according to

$$|\rho^*| = \sqrt{\frac{1}{(\sigma')^2 + (\sigma'')^2}} \quad (3)$$

and

$$\arctan(\varphi) = -\frac{\sigma''}{\sigma'} \quad (4)$$

The frequency dependence of the complex conductivity of rocks at very low frequencies is also the basis of Induced Polarisation measurements. The frequency effect FE (Parasnis, 1966) is an easily measurable quantity describing the fractional

decrease of the resistivity magnitude with increasing frequency ω :

$$FE = \frac{|\rho^*(\omega_1) - |\rho^*(\omega_2)|}{|\rho^*(\omega_2)|} \quad (5)$$

The frequency effect FE is related to the phase angle φ :

$$FE = \text{const.} \cdot \varphi \quad (6)$$

Vinegar and Waxman (1984) showed for a group of shaly sandstones the validity of equation.

EXPERIMENTAL

Measurement system

The complex conductivities were measured with a laboratory system (Figure 1), similar to but less sophisticated than the low frequency part of the equipment used by Olhoeft (1979). The measurements were made at frequencies between 10^{-3} and 10^4 Hz, which includes the common IP-frequency range.

Measurements were carried out at room conditions (normal pressure and 25 °C). The cylindrical samples (plugs, 20 mm diameter and 30 mm length) were sealed with a teflon bandage and pressed into a plastic jacket.

As shown in Figure 2, the four-electrode-measuring-cell consists of two reservoirs for electrolyte solution, connected with the cased plug. For the electrodes platinum mesh has been used. The potential electrodes are placed at the sample surface separated by a thin inert membrane only, while the current electrodes are immersed into the solution filled reservoirs.

A measuring system has been used consisting of a computer controlled signal source and a digital storage oscilloscope. The stimulus current is measured in a first channel by recording the voltage drop across a resistor in series to the measuring

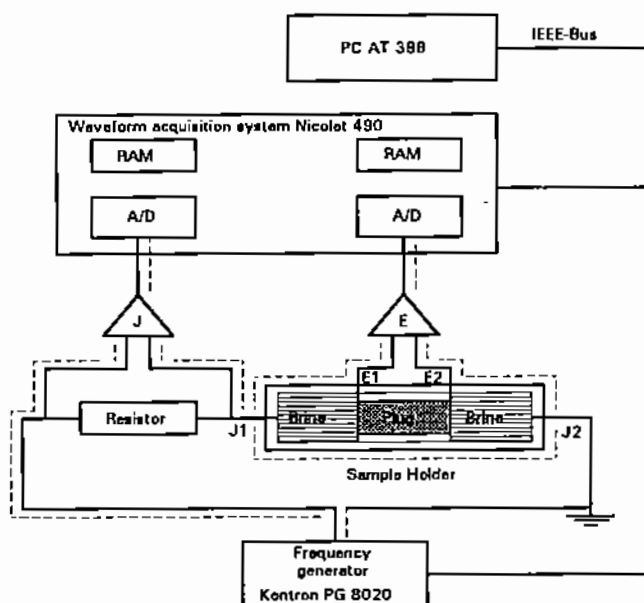


FIGURE 1 Scheme of the simple low frequency measurement system (Trade names are used for illustrative purposes only).

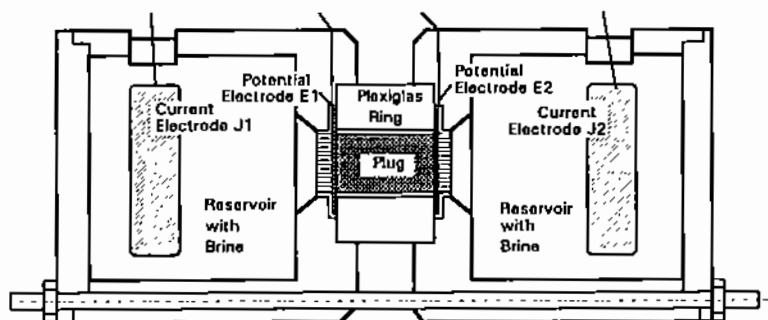


FIGURE 2 Four-Electrode-Measuring Cell.

cell. The resulting voltage drop across the sample length is recorded in a second channel. Very high input impedance amplifiers protect the system from effects of electrode polarization and coupling between the two channels. After synchronous digitalisation and summarization the two time series (current, voltage) are processed with a linear inversion algorithm according to Olhoeft (1979). The calibration was made using standard resistors and materials with neglecting polarization effects (brine, saturated porous ceramic).

Sample Preparation

Complex conductivity measurements were made on a series of 28 different sandstone samples. The sample specification including a short geological description can be seen in Table 1. The porosity Φ , grain density d_m , internal surface area S_m and the surface to porosity ratio S_{por} have been used to characterize the material. Porosity and density were measured by water injection on samples with a defined geometry. Internal surface area S_m was determined by using BET-nitrogen-adsorption. The relation to the parameter S_{por} , which is important for transport properties of rocks (Engelhardt, 1960) is given by

$$S_{por} = \frac{S_m d_m (1 - \Phi)}{\Phi} \quad (7)$$

Additionally, the gas permeability was measured at a number of samples. All samples were saturated with sodium chloride solution of known conductivity σ_w at 25°C after drying at 60°C to a constant weight. All samples were saturated with a brine which have a conductivity of about 0.1 S/m. The final value for σ_w was determined from a measurement immediately before and after the detection of frequency dependence. A series of selected sandstone samples was saturated with brine of different conductivities.

The contaminating organic substances were added to the samples which then were hermetically sealed. After an interaction time of two months the preparation was continued with the saturation using sodium chloride solution. Inorganic contamination was simulated using solutions of different chlorides.

TABLE 1 Petrophysical properties (Typical samples).

Sample	Location	Φ (-)	S_{por} (μm^{-1})	S_m ($10^3 \text{ m}^2/\text{kg}$)	k_{gas} ($10^{-3} \mu\text{m}^2$)
E6	Saxony	0.1980	31.1	2.96	-
E7	(Germany)	0.2762	13.2	1.95	157
E10		0.2238	41.6	4.64	5.4
E12		0.2589	5.5	0.748	1490
E14		0.2403	10.7	1.31	1990
E17		0.1806	1.44	0.122	680
B2	Bentheim	0.1943	2.15	0.198	1880
B4	(Germany)	0.2315	2.22	0.261 ^a	-
R1	Altmark	0.0463	43.5	0.809	-
R3	(Germany)	0.0970	24.7	1.01	0.52
F1	Fontainebleau	0.2143	0.146	0.0153 ^a	-
F3	(France)	0.0676	0.126	0.0036 ^a	138

^a Data from Clausthal University/Germany

TABLE 2 Complex electrical parameters of sandstones, saturated with brine (Typical Results for $\sigma_w = 0.1 \text{ S/m}$).

Sample	σ'_n (S/m)	σ''_n (S/m)	P (-)
E6	0.0129	0.000294	0.9853
E7	0.0170	0.000247	0.9909
E10	0.0185	0.000275	0.9903
E12	0.00861	0.0000829	0.9950
E14	0.00958	0.0000778	0.9947
E17	0.00374	0.0000114	0.9979
B2	0.0157	0.000018	0.9991
B4	0.00763	0.000044	0.9963
R1	0.0396	0.000127	0.9978
R3	0.0107	0.000144	0.9924
F1	0.00762	0.00000302	0.9997
F3	0.000719	0.00000184	0.9983

Partially saturated samples have been analysed using a modified four-electrode arrangement (brine saturated ceramic in place of the brine filled reservoirs). Saturations were established by spontaneous imbibition or centrifuging and controlled by weighing. The adjustment to a constant fluid distribution within the plug was controlled by resistivity measurement. Constant values were established after approximately 2 hours. Subsequently the sample was cased and built into the measuring cell. S_w measurements were made before and after the IP-measurements. They were accepted if the error from the two S_w determinations was less than 5 %.

EXPERIMENTAL RESULTS

General Frequency Dependence

Figure 3 illustrates the measured frequency dependence of complex conductivity of a Bentheim sandstone in the range from 10^{-3} to 10^4 Hz. The nearly identical power law dependence of the real as well as the imaginary part on frequency is the main feature observed. This behaviour of the conductivity is caused by a nearly constant negative phase angle over more than 6 decades of frequency and an accompanying steady decrease of the resistivity magnitude with increasing frequency.

All investigated samples of clean and shaly sandstones show in general such a frequency behaviour of conductivity. Based on the constant phase angle behaviour (Jonscher, 1981) the general dependence of complex conductivity σ^* on frequency in the range from 10^{-3} to 10^4 Hz can be well expressed with an empirical power law:

$$\sigma^*(\omega) = \sigma_n (i\omega_n)^{1-p} \quad (8)$$

where σ_n is an amplitude factor, ω_n the angular frequency, normalized to $\omega = 1 \text{ s}^{-1}$. $1-p$ is a frequency exponent in the

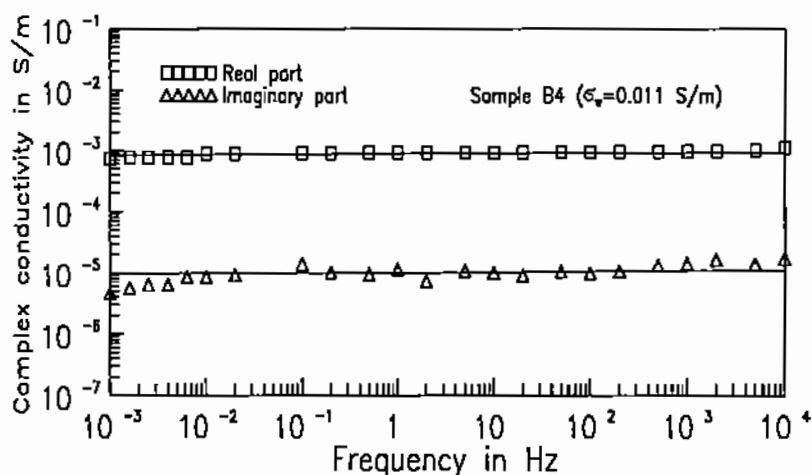


FIGURE 3 Frequency dependence of real and imaginary part of the complex conductivity.

order of 0 to 0.03. The best fit according to equation (8) is plotted additionally in Figure 3. This behaviour is identical with the low frequency portion of the Anomalous low frequency dispersion model developed by Dissado and Hill (1984). According to this model the dispersion is connected with a process of charge carrier hopping at the surface of water adsorbing systems. At low frequencies this process appears as an intercluster motion. The interface has an integrated influence on charge transport, thus larger structures in the pore space are important for electrical behaviour in this frequency range. In this sense a cluster is a group of charge carriers determined by the pore space geometry.

The constant phase angle behaviour changes to a Cole-Cole-behaviour for the conductivity at frequencies higher than 10 kHz. (Kulenkampff and Schopper, 1988, Ruffet et al., 1991). The connection of the constant phase angle behaviour according to equation (8) and the Cole-Cole-behaviour at higher frequencies enables the analysis of complex conductivity with

one equation between 10^{-3} and 10^6 Hz to be made (Börner and Kulenkampff, 1992).

The following two expressions have been used for the description of experimental data in the investigated frequency range (10^{-3} - 10^4 Hz):

$$\sigma'(\omega) = \sigma'_n \omega_n^{1-p} \quad (9a)$$

$$\sigma''(\omega) = \sigma''_n \omega_n^{1-p} \quad (9b)$$

σ'_n and σ''_n are frequency independent prefactors of the real and imaginary part of conductivity, equal to σ' and σ'' at $\omega = 1$ Hz.

The term ω_n^{1-p} describes the frequency dependence. The separation of (8) into real and imaginary part leads to the relationship between the frequency exponent $1-p$, the phase angle φ and the parameters in equation (9a,b):

$$\tan \varphi = -\frac{\sigma''_n}{\sigma'_n} = \tan \left[\frac{\pi}{2} (1-p) \right] \quad (10)$$

σ'_n , σ''_n and p have been obtained by regression of σ' and σ'' vs. ω (Table 2). The validity of formula (10) was tested by plotting p , calculated from φ vs. p , obtained by regression (see Figure 4). The electrical conductivity of wet porous rocks is mainly related to the fluid properties and pore space geometry. Porosity and specific surface area are important textural parameters that are related to fluid flow in rocks. Interactions between mineral matrix and pore fluid and the distributed nature of pore space geometry are responsible for the capacitive behaviour and the frequency dependence of electrical parameters of the rock.

Vinegar and Waxman (1984) developed a complex conductivity model based on the Waxman-Smits-concept of cation exchange capacity as shalyness parameter (Waxman and Smits, 1968). Its validity is limited to the frequency range from 3 Hz to 3 kHz and the frequency dependence of complex conductivity components (equation 8) have not been shown

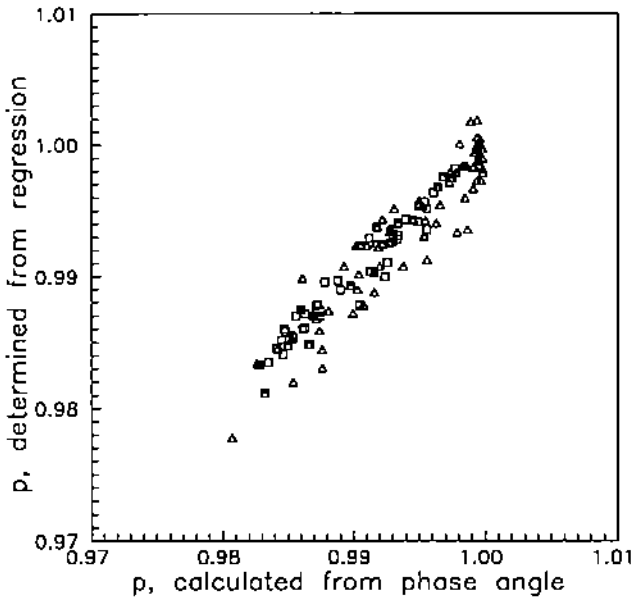


FIGURE 4 p from Regression vs. p calculated from ϕ .

explicitly in their analysis. The present analysis considers the frequency dependence between 10^{-3} and 10^4 Hz.

For better understanding of the conductivity dispersion the relationship between the parameters in equation (9a,b) and some reservoir properties has been analysed.

Relationship to Pore Space Geometry

The experimental investigation of salinity dependence of complex conductivity has shown that σ_n in equation (8) consists of a real electrolytical volume (σ_{el}) and a complex interface conductivity (σ'_i). The prefactor of the real part σ'_n in equation (9a) is then composed of σ_{el} and the real part of the interface conductivity σ'_i , corresponding to the expression of

Rink and Schopper (1974) for fixed frequency measurements:

$$\sigma'_n = \sigma_{el} + \sigma'_i \quad (11)$$

The prefactor of the imaginary part σ''_n in equation (9b) is identical with the imaginary part of a complex interface conductivity σ''_i in the low frequency range:

$$\sigma''_n = \sigma''_i \quad (12)$$

This shows that the complex nature of conductivity at frequencies lower than 10 kHz is caused by a complex interface conductivity only. This is physically plausible, because the capacitive behaviour is caused solely by interaction effects between nonconductive matrix and brine, which results in development of an electrical double layer. A typical example of salinity dependence of complex conductivity components is given in Figure 5.

The experimental results in Figure 6 show that both interface conductivity components are linear dependent on S_{por} (Börner and Schön, 1991). Furthermore, they show nearly the same type of dependence on water salinity (see Figure 5). Therefore, they are supposed to be parts of a complex interface conductivity caused by one electrical mechanism which creating an ohmic and a capacitive conductivity component.

σ_{el} in (11) is identical with the well known Archie-equation (Archie, 1942, Schön, 1983) and proportional to porosity Φ :

$$\sigma_{el} = \frac{\sigma_w}{F}, \frac{1}{F} \propto \Phi \quad (13)$$

where F is the true (high salinity) formation factor and σ_w the electrolyte conductivity.

Various methods are used to express the second term in equation (11) for fixed frequency conditions (Waxman and Smits, 1968, Clavier et al., 1977, Pape and Worthington, 1983, Börner and Schön, 1987 or Sen et al., 1988). A summary is given in Worthington (1986).

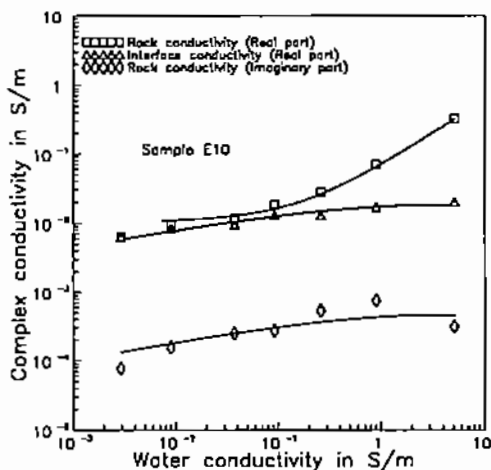


FIGURE 5 Variation of Complex Conductivity Components with Electrolyte Conductivity σ_w .

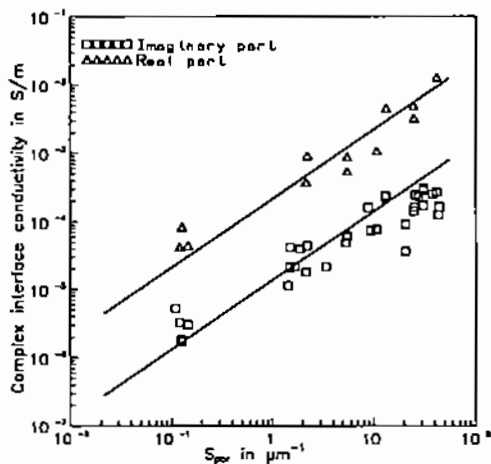


FIGURE 6 Complex Interface Conductivity Components vs. Surface-to-Porosity ratio S_{por} .

Based on Rink and Schopper's (1974) equation, σ'_i is described as

$$\sigma'_i = \frac{f(\sigma_w)S_{por}}{F} \quad (14)$$

where F , for purposes of simplicity, is the same formation factor as in equation (13) and $f(\sigma_w)$ is a general function considering salinity dependence. It was found that the ratio of the two interface conductivity components l ,

$$l = \frac{\sigma''_i}{\sigma'_i} \quad (15)$$

is nearly independent on salinity but slightly different in various types of sandstones (see Table. 3). Combination of equations (15) and (14) yields an expression for the imaginary part of interface conductivity (Börner, 1991):

$$\sigma''_i = \frac{l f(\sigma_w) S_{por}}{F} \quad (16)$$

l being in the order of 0.01 to 0.15. Ratio l seems to be related

TABLE 3 Electrical parameters (Multiple salinity method).

Sample	F	$\sigma'_i (\sigma_w \rightarrow \infty)$ (S/m)	$\sigma''_i (\sigma_w \rightarrow \infty)$ (S/m)	$l = \sigma''_i / \sigma'_i$ (-)
E10	17.0	0.021	0.0008	0.0286±0.0123
E12	11.0	0.0018	0.00025	0.101±0.033
E14	11.1	0.003	0.00027	0.0605±0.017
B2	15.6	0.0007	0.000037	0.0511±0.0176
F1	12.5	0.0001	0.000008	0.0579±0.0404
F3	118	0.0002	0.000005	0.0236±0.00904
R3	45.1	0.008	0.00035	0.0276±0.0118

to the product of porosity and formation factor (Figure 7), which in turn is related to tortuosity and constrictivity of pore space (PAPE et al., 1987).

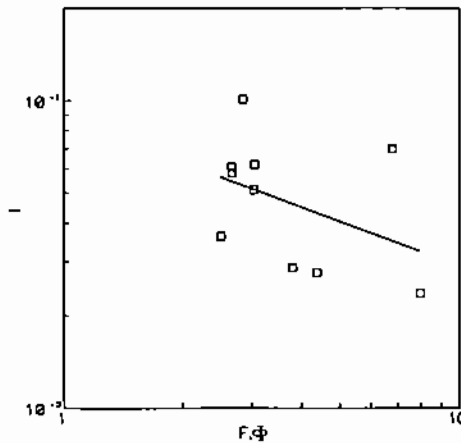


FIGURE 7 Variation of the Ratio I with the Product $F \cdot \Phi$.

Relationship to Water Salinity

The observed salinity dependence of complex interface conductivity components did not show any significant changes in I with varying water conductivity (Table 4). This means, a variation of the ionic concentration in the liquid phase influences the interphase properties (e.g. double layer thickness, charge density) and consequently the entire conduction mechanism with its ohmic and capacitive components. Waxman and Smits (1968) and Vinegar and Waxman (1984) derived empirical expressions with a salinity dependent cation mobility. Stenson and Sharma (1989) showed that the charge density in the grain-electrolyte interphase is influenced by salinity too.

TABLE 4 Complex electrical parameters for the investigated sandstones (selected Samples), saturated with NaCl-solution of different salinities.

Sample	σ_w	σ'_n	σ'_i	σ''_i	ρ	$l = \sigma''_i/\sigma'_i$
	(S/m)	(S/m)	(S/m)	(S/m)	(-)	(-)
E10	0.0029	0.00644	0.00827	0.000078	0.9904	0.0124
	0.0090	0.00846	0.00847	0.000156	0.9878	0.0184
	0.0373	0.0116	0.00941	0.00025	0.9861	0.0266
	0.0921	0.0185	0.0131	0.000275	0.9903	0.0210
	0.26	0.0281	0.0128	0.000535	0.9876	0.0418
	0.897	0.0697	0.0169	0.000751	0.9922	0.0444
	5.1	0.324	0.0199	0.000709	0.9990	0.0356
E12	0.0031	0.000574	0.000292	0.0000149	0.9822	0.0510
	0.0093	0.00109	0.000244	0.0000249	0.9837	0.102
	0.0359	0.00362	0.000356	0.0000510	0.9908	0.143
	0.0886	0.00861	0.000555	0.0000629	0.9950	0.113
	0.0902	0.00909	0.000890	0.0000611	0.9954	0.0686
	0.221	0.0212	0.00111	0.0000995	0.9969	0.0896
	0.936	0.0866	0.00151	0.000142	0.9989	0.0940
	5.11	0.466	0.00145	0.00021	0.9996	0.145
B2	0.0032	0.000376	0.000171	0.00000622	0.9897	0.0364
	0.0100	0.000744	0.000103	0.00000835	0.9931	0.0811
	0.0335	0.00234	0.000192	0.0000117	0.9967	0.0609
	0.239	0.157	0.000379	0.000018	0.9991	0.0475
	0.935	0.0605	0.000564	0.0000265	0.9996	0.0470
	5.34	0.343	0.000692	0.0000232	1.0	0.0335
F3	0.0016	0.000088	0.0000753	0.00000122	0.9910	0.0162
	0.0107	0.000134	0.0000433	0.00000148	0.9928	0.0342
	0.0103	0.000157	0.0000697	0.00000202	0.9916	0.0289
	0.0157	0.000186	0.0000529	0.00000156	0.9946	0.0295
	0.0752	0.000719	0.0000817	0.00000184	0.9983	0.0225
	1.12	0.00965	0.000158	0.00000414	0.9997	0.0262
	1.6	0.014	0.000441	0.0000034	0.9998	0.0077

Salinity dependence $f(\sigma_w)$ is assumed to be caused by a medium charge density $\alpha(\sigma_w)$ in the interphase region only, the cation mobility β being a constant:

$$f(\sigma_w) = \alpha(\sigma_w)\beta \quad (17)$$

The application of the model of a simple plate capacitor to the interphase region (Kulenkampff and Schopper, 1988) with a constant Stern layer thickness and a Gouy layer (diffuse layer) thickness, which is inversely proportional to salinity, yields to a square root dependence of the charge density in a smoothed interphase region. $\alpha(\sigma_w)$ decreases with deminishing salinity according to

$$\alpha(\sigma_w) \propto \frac{\sqrt{\sigma_w}}{1 + \sqrt{\sigma_w}} \quad (18)$$

The experimental data of the samples verify the increase of the complex interface conductivity with a power of about 0.5 at medium salinities, which results from the double layer theory. At high salinities $f(\sigma_w)$ becomes a constant value equal to the product of constant charge density and cation mobility (about 9 nS, Riepe et al., 1979). $f(\sigma_w)$ is then

$$f(\sigma_w) = \frac{\alpha\beta}{c_1 + (c_2\sigma_w)^{-0.5}} \quad (19)$$

The parameters c_1 and c_2 are connected with the salinity dependent double layer thickness, the fluid permittivity, temperature, the surface potential and other quantities.

Relationship to IP-Measurements

The increase of conductivity with increasing frequency is related to the frequency exponent $1-p$ and consequently to the constant phase angle behaviour. The so called "logarithmic frequency effect" LFE, obtained from regression of $\log[\sigma^*(\omega)]$ vs. $\log[\omega]$,

$$LFE = \frac{\partial \lg[\sigma^*(\omega)]}{\partial \lg(\omega)} \quad (20)$$

is clearly related to the constant phase angle and valid over the whole of the investigated frequency range (Figure 8). In its simplest case, it is obtained from conductivity measurements at two different frequencies:

$$LFE = \frac{\lg[\sigma^*(\omega_2)] - \lg[\sigma^*(\omega_1)]}{\lg(\omega_2) - \lg(\omega_1)} \quad (21)$$

LFE and $1-p$, respectively, are described using terms for real and imaginary parts of conductivity obtained from equations (11) to (16):

$$\sigma'_n = \frac{1}{F} [\sigma_w + f(\sigma_w) S_{por}] \quad (22a)$$

$$\sigma''_n = \frac{1}{F} f(\sigma_w) l S_{por} \quad (22b)$$

Using these two expressions the equation for the frequency effect of a brine saturated sandstone becomes

$$LFE = 1 - p = \frac{2 \frac{1}{F} f(\sigma_w) l S_{por}}{\pi \frac{1}{F} [\sigma_w + f(\sigma_w) S_{por}]} \quad (23)$$

When equation (23) and the equation for the salinity dependence of interface conductivity (19) are combined, LFE is

$$LFE = 1 - p = \frac{2}{\pi} \left[\frac{\sigma_w (c_1 + l / \sqrt{c_2 \sigma_w})}{\alpha \beta S_{por}} + \frac{1}{l} \right]^{-1} = \frac{2}{\pi} \left[\frac{f'(\sigma_w)}{\alpha \beta S_{por}} + \frac{1}{l} \right]^{-1} \quad (24)$$

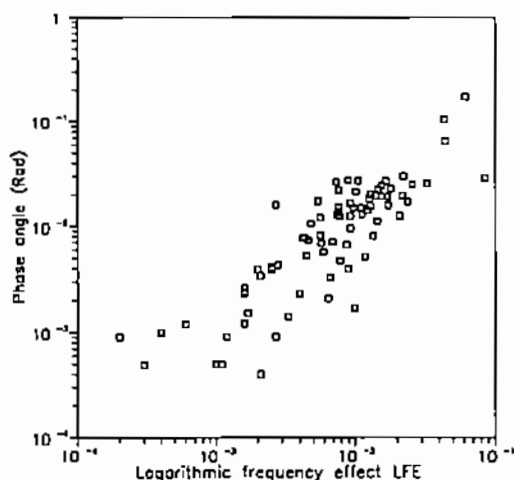


FIGURE 8 Phase angle vs. logarithmic frequency effect

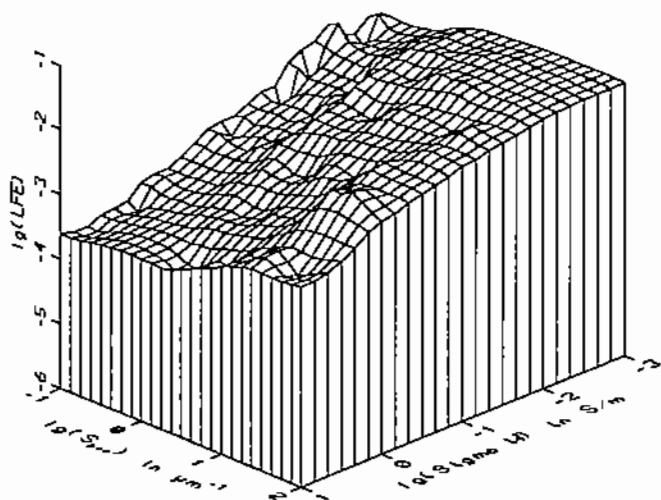
This relationship between the frequency dependence (LFE, $1-p$ or phase angle, respectively) on the one hand, and the pore space structure (S_{por} , l) and water salinity $f'(\sigma_w)$ on the other, is strictly based on the (1) constant phase angle behaviour and (2) the salinity independent ratio of surface conductivity components. The limiting behaviour for high and low water salinity and high and low S_{por} -values results from equation (24):

$$p(\sigma_w \rightarrow 0, S_{por} \rightarrow \infty) = 1 - \frac{\pi}{2}l \quad (25a)$$

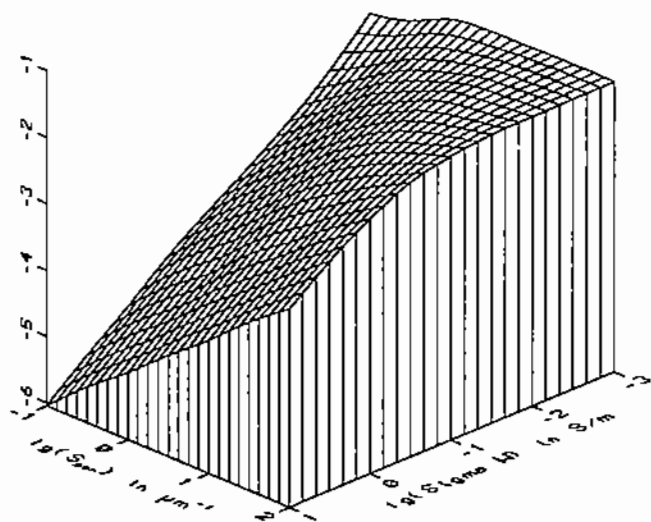
$$p(\sigma_w \rightarrow \infty, S_{por} \rightarrow 0) = 1 \quad (25b)$$

Experimental and calculated results of the dependence of LFE on S_{por} and on electrolyt conductivity σ_w are shown in 3D-plots in Figure 9.

It is possible to obtain the real and imaginary part of conductivity for practical applications on the basis of the measured conductivity magnitude and its frequency dependence. Since the imaginary part is very small in comparison to the real part,



A



B

FIGURE 9 Variation of LFE with water conductivity σ_w and surface-to-porosity-ratio S_{por} : (A) experimental results, (B) calculated using formula (24).

σ'_i is nearly identical with the measured conductivity magnitude σ_n . From equations (8) and (9) follows

$$\sigma_n \approx \sigma'_n = \sigma_n \cos \left[(1-p) \frac{\pi}{2} \right] \quad (26)$$

and for the imaginary part σ''_i

$$\sigma''_n = \sigma_n \sin \left[(1-p) \frac{\pi}{2} \right] \quad (27)$$

For a given formation l is nearly a constant. Therefore, the real part of interface conductivity can be calculated from the imaginary part

$$\sigma'_i = \frac{\sigma''_i}{l} \quad (28)$$

and then σ'_n can be divided into the volume and the real interface conductivity component. By using brine conductivity the true formation factor F is obtained. On the other hand, if porosity is determined independently, brine conductivity can be calculated.

Partially Water saturated Samples

The analysis of the dependence of complex electrical conductivity on water saturation is important for determining of oil and gas saturation or evaluating aerated soil zone in connection with ground water problems. As the measurement of partially saturated plugs at very low frequencies is very complicated, only a limited first set of data is available.

i^* is the saturation index derived from the imaginary part of complex rock conductivity (Vinegar and Waxman, 1984):

$$i^*(S_w) = \frac{\sigma''_n(S_w)}{\sigma''_n(S_w = 1)} \quad (29)$$

Figure 10 shows the decrease of i^* with decreasing water

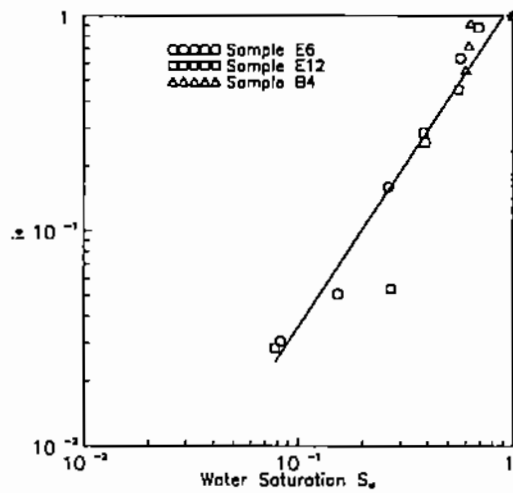


FIGURE 10 Variation of i^* with Water Saturation.

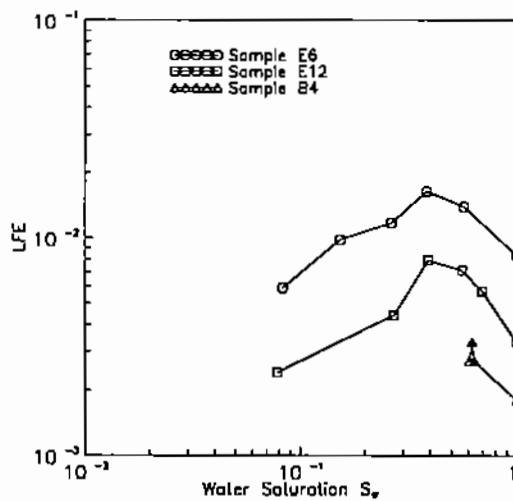


FIGURE 11 Variation of LFE with Water Saturation.

saturation for three samples which are different in their S_{por} -values. The dependence of the frequency exponent on water saturation for the sample E6 is plotted in Figure 11. LFE shows a complicated relationship to S_w . It seems that the initial increase of frequency dependence is caused by the significant decrease of the electrolytic volume conductivity. The shape of the curve at S_w -values lower than 0.5 is controlled by the complex interface conductivity. For more general conclusions some further experiments are necessary.

Organic and inorganic Contaminants

The complex interface conductivity is influenced by changes of composition of the pore fluid and accompanying physico-chemical processes resulting in changes of the interphase microstructure. The interface region of a rock or soil can be expected to be very sensitive to changes in material composition caused by organic and inorganic contamination. As a contribution to a better understanding of electrical rock properties as well as to the problem of contamination indication the complex electrical behaviour in the low frequency range of artificially contaminated samples has been studied.

The first example shows the variation of the frequency exponent $1-p$ (or LFE resp.) with varying amounts of a polar organic substance in pore water. The sample was contaminated with methanol (CH_3OH , dielectric constant = 34) of different saturation degrees. The actual pore fluid conductivity was nearly constant and about equal to the conductivity of pure methanol. The measured frequency dependence vs. methanol saturation is shown in Figure 12. A similar behaviour was found for the contaminants hexane, dichlormethane, benzene, toluene and others. The frequency dependence decreases with increasing percentage content and decreasing dielectric constant of the contaminant. In order to investigate the influence of different salt types some sandstones were saturated with chlorides of different cations (Gruhne and Börner, 1992). Different mobilities and cation radii cause deviations in the frequency dependence of conductivity (Figure 13).

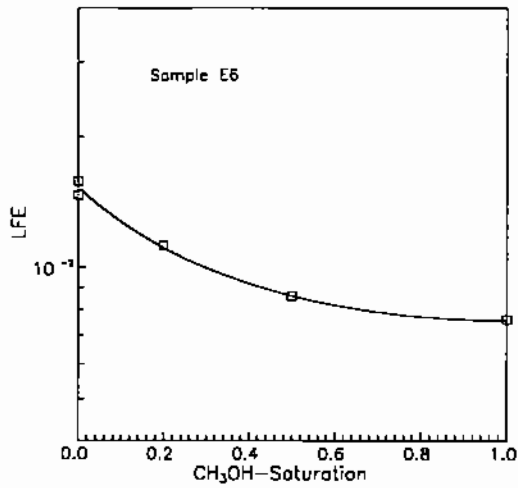


FIGURE 12 Variation of LFE with Contaminant Saturation.

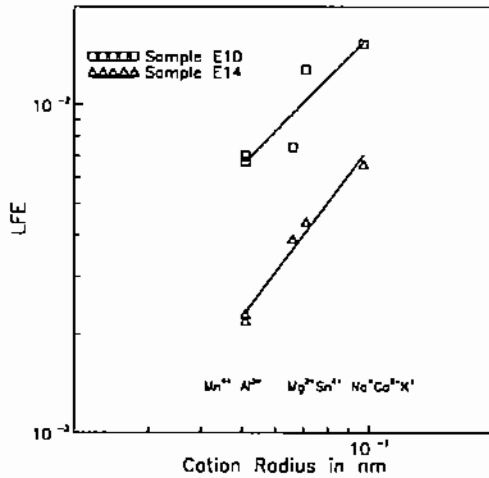


FIGURE 13 Variation of LFE with Cation Type, experimental results for NaCl, MgCl₂, AlCl₃ and SnCl₄.

CONCLUSIONS

Experimental investigation of clean and shaly sandstones in the frequency range from 10^{-3} to 10^4 Hz show that the frequency dependence of electrical conductivity is caused by a complex interface conductivity. Its components, the real as well as the imaginary part, show (1) a linear dependence on the surface to porosity ratio S_{por} , and (2) a weak increase with increasing water salinity and (3) a nearly salinity independent ratio of the two components.

On this basis the experimentally measured frequency dependence for water saturated rocks was described with a relatively simple equation, which includes a real electrolytic volume conductivity and a complex interface conductivity. The defined logarithmic frequency effect is a measure which can be obtained for practical purposes from IP-measurements. The application of the equation to field measurements enables the internal surface area to be calculated from the measured conductivity magnitude and frequency dependence. Further investigations are necessary to get more information about the relationship of low frequency complex conductivity and water saturation as well as amount and properties of contaminants.

ACKNOWLEDGEMENTS

Parts of this work has been supported by the Volkswagenstiftung (Germany). The author expresses his thanks to J. Schön (Leoben, Austria), and J.R. Schopper and the Clausthal Petrophysical group (Clausthal, Germany) for many useful discussions and providing petrophysical core analysis.

REFERENCES

ARCHIE, G.E. (1942) The electrical resistivity log as an aid in determining some reservoir characteristics. *Transactions of the American Institute of Mining, Metallurgical and Petroleum Engineers*, 146, 54-62

BÖRNER, F.D. and SCHÖN, J.H. (1987) Experimental investigation of the electrical conductivity of unconsolidated rocks. In *Proceedings of the 32nd International Geophysical Symposium* (Dresden, 1987), edited by H. Thieme, pp. 151-159 Leipzig: Kombinat Geophysik

BÖRNER, F.D. (1991) Investigation of the complex electrical conductivity between 1 mHz and 10 kHz. *Dr. Thesis*, Mining Academy Freiberg, Freiberg, Germany

BÖRNER, F.D. and SCHÖN, J.H. (1991) A relation between the quadrature component of electrical conductivity and the specific surface area of sedimentary rocks. *The Log Analyst*, **32**, 612-613

BÖRNER, F.D. and KULENKAMPPF, J. (1992) The Dispersion of the Complex Electrical Conductivity between 0.001 Hz and 1 MHz. In *Proceedings of the 52nd Annual Meeting of the German Geophysical Society* (Leipzig, 1992), p. 164

CLAVIER, C., COATES, G. and DUMANOIR, J. (1977) Theoretical and experimental basis for the "Dual water" model for interpretation of shaly sands. In *Proceedings of the 52nd Annual Technical Conference and Exhibition of the Society of Petroleum Engineers* (Denver, 1977), paper SPE 6859

DISSADO, L. and HILL, R.M. (1984) Anomalous low frequency dispersion. *J. Chem. Soc. Faraday Trans.*, **80**, 291-319

ENGELHARDT, W. v. (1960) *Der Porenraum der Sedimente*, 1st edn, Berlin, Göttingen, Heidelberg: Springer Publishers

GRUHNE, M. and BÖRNER, F.D. (1992) Complex conductivity used for contamination indication. In *Proceedings of the 52nd Annual Meeting of the German Geophysical Society* (Leipzig, 1992), p. 160

JONSCHER, A.K. (1981) A new understanding of the dielectric relaxation of solids. *Journal of Material Sciences*, **16**, 2037-2060

KULENKAMPFF, J. und SCHOPPER, J.R. (1988) Low frequency complex conductivity - a means for separating volume and interlayer conductivity. In *Transactions of the 12th European Formation Evaluation Symposium* (Oslo, 1988)

LOCKNER, D.A. and BYERLEE, J.D. (1985) Complex resistivity measurements of confined rock. *Journal of Geophysical Research*, **90**, 7837-7847

OLHOEFT, G.R. (1979) Electrical properties. Initial Reports on the Petrophysics Laboratory. *U.S. Geological Survey Circular*, **789**, 1-26

OLHOEFT, G.R. (1985) Low frequency electrical properties. *Geophysics*, **50**, 2492-2503

PAPE, H., RIEPE, L. and SCHOPPER, J.R. (1987) Theory of self-similar network structures in sedimentary and igneous rocks and their investigation with microscopical and physical methods. *Journal of Microscopy*, **148**, 121-147

PAPE, H. and WORTHINGTON, P.F. (1983) A surface structure model for the electrical conductivity of reservoir rocks. In *Transactions of the 8th European Formation Evaluation Symposium* (London, 1983), Z1-Z19

PARASNIS, D.S. (1966) *Mining Geophysics*. Amsterdam, New York: Elsevier Publishers

RIEPE, L., RINK, M. and SCHOPPER, J.R. (1979) Relations between specific surface dependent rock properties. In *Transactions of the 6th European Logging Symposium* (London, 1979)

RINK, M., and SCHOPPER, J.R. (1974) Interface conductivity and its implication to electric logging. In *Transactions of the 15th Annual Logging Symposium* (London, 1974)

RUFFET, C., GUEGUEN, Y. and DAROT, M. (1991) Complex conductivity measurements and fractal nature of porosity. *Geophysics*, **56**, 758-768

SCHÖN, J. (1983) *Petrophysik*. 1st. edn, Berlin: Akademie-Publishers

SEN, P.N., GOODE, P.A. and SIBBIT, A. (1988) Electrical conduction in clay bearing sandstones at low and high salinities. *Journal of Applied Physics*, **63**, 4832-4840

STENSON, J.D. and SHARMA, M.M. (1989) A petrophysical model for shaly sands. In *Proceedings of the 64th Annual Technical Conference and Exhibition of the Society of Petroleum Engineers* (San Antonio, 1989), paper SPE 19574

VINEGAR, H.J. and WAXMAN, M.H. (1984) Induced Polarization of Shaly Sands. *Geophysics* **49**, 1267-1287

WAXMAN, M.H. and SMITS, L.J.M. (1968) Electrical Conductivities in oil-bearing Shaly Sands. *Society of Petroleum Engineers Journal*, **243**, 107-122

WILEY, R. und SNOODY, M.L. (1986) Complex resistivity of shaly sands and minerals. *The Log Analyst*, **27**, 45-49

WORTHINGTON, P.F. (1986) The relationship of aquifer petrophysics to hydrocarbon evaluation. *Quarterly Journal of Engineering Geology*, London, **19**, 97-107